

N66 24633

26. COMPARISON OF WIND-TUNNEL AND FLIGHT-TEST AERODYNAMIC
DATA IN THE TRANSITION-FLIGHT SPEED RANGE FOR

FIVE V/STOL AIRCRAFT*

By Woodrow L. Cook and David H. Hickey
Ames Research Center

SUMMARY

24633

Four aircraft and one large-scale model which represent the V/STOL spectrum from low-disk-loading rotocraft to high-disk-loading lift-fan systems have been studied in the Ames Research Center's 40- by 80-Foot Wind Tunnel. In general, the aircraft were tested in the wind tunnel near trimmed, level-flight conditions. The power required, angle of attack, and control positions for the appropriate flight conditions as measured in the wind tunnel are compared with flight-test results. Agreement between wind-tunnel and flight-test measurements was generally good when wind-tunnel wall corrections were omitted. The aircraft and wind-tunnel geometry is related to wind-tunnel model sizing parameters and a VTOL lift parameter in order to establish tentative sizing criteria for V/STOL wind-tunnel testing with small wall effects.

INTRODUCTION

Author

For the advancement of the V/STOL state of the art and the development of useful V/STOL concepts and configurations, it is essential to have correct wind-tunnel test data. Very little experimental information is available for defining acceptable geometric relationships between models and wind tunnels or the momentum relationships between the propulsive and lift forces and the wind-tunnel air flow necessary for keeping wall effects small in wind-tunnel test data for the transition speed range of V/STOL type aircraft. The jet-boundary effects for V/STOL wind-tunnel tests are complex, and although the theoretical treatment of reference 1 represents an advancement in determining these effects, more accurate methods are being developed. The theory of reference 1 has been verified experimentally for helicopter rotors with low disk loadings (ref. 2). To determine wall effects of V/STOL concepts with higher disk loadings, a single model was tested in various sized wind tunnels (refs. 3-5) and the measured wall corrections were correlated with those calculated by the method of reference 1.

26

In order to predict the aerodynamic characteristics of V/STOL aircraft, it is often necessary to compromise the ideal ratio of model size to tunnel size required for data with small wall effects for a number of reasons, including the Reynolds number of the model and the propulsion system components, the

*Presented at AGARD Flight Mechanics Panel, Rome, Italy, Oct. 12, 1965.

requirement for tests of full-scale airplane hardware in large wind tunnels, and difficulties involved in designing and constructing of propulsion system hardware for small wind tunnels.

In this report the effect of wall constraints are examined by correlating the aerodynamic characteristics of wind-tunnel and flight investigations for four aircraft and one large-scale model representing several V/STOL concepts. In an attempt to provide some insight into the order of magnitude of model size to wind-tunnel size ratio, tentative boundaries for three sizing parameters are also presented, based on the correlation of flight results to wind-tunnel data.

NOMENCLATURE

A_L	area of VTOL lifting element, $n(\pi D_L^2/4)$, sq ft
A_M	momentum area of aircraft, $\pi b^2/4$, sq ft
A_T	wind-tunnel cross-section area, sq ft
b	wing span, ft
b_T	tunnel width, ft
D_L	diameter of lifting element, ft
h_T	tunnel height, ft
i_w	wing incidence angle, deg
L	lift, lb
n	number of propellers, fans, or rotors
T_F	fan thrust, lb
V	airspeed, knots
V_j	jet velocity, knots
δ_f	flap deflection angle, deg

DESCRIPTION OF TEST AIRCRAFT

Aircraft dimensions pertinent to the calculation of wind-tunnel wall corrections are presented in table I. Further details of the individual aircraft follow.

Bell XV-3

The XV-3 shown in figure 1 has a 23-foot-diameter helicopter rotor mounted on a mast at each wing tip. While hovering, the aircraft functions as a helicopter with helicopter-type controls. In order to attain wing-supported flight speed, the rotor masts are tilted forward until the rotor axes are aligned with the flight path. Further details of this aircraft are given in reference 6.

Ryan VZ-3

The VZ-3 (fig. 2) uses an extensive flap system to deflect the propeller slipstream downward to attain VTOL capability. The VTOL controls consist of a combination of propeller-pitch controls, wing-mounted controls in the propeller slipstream, and reaction control from the thrust of the turboshaft engine. The transition from hover to conventional flight is accomplished by decreasing the flap deflection (and thus the propeller slipstream deflection) to provide thrust for acceleration. Further details of this aircraft are presented in reference 7.

Chance Vought-Ryan-Hiller XC-142

The XC-142 (the 0.6-scale model tested in the wind tunnel is shown in fig. 3) is a tilt-wing aircraft with four engines and four propellers. The aircraft uses full-span flaps to help deflect the propeller slipstream and reduce the wing tilt required. Hover controls consist of variable-pitch propeller controls, controls mounted on the wing in the propeller slipstream, and a tail-mounted rotor for pitch control. Speed for wing-supported flight is obtained by reducing wing tilt and flap deflection. Wind-tunnel data presented herein are from the 0.6-scale model (ref. 8). Model power limitations caused the test airspeed to be reduced to about one-half of the full-scale value.

Lockheed XV-4A

The XV-4A (fig. 4) is powered by two jet engines which exhaust vertically through an ejector in the fuselage for VTOL lift and exhaust normally for cruise thrust. Hover, pitch, and yaw control are supplied by the reaction from tail-pipe bleed, and roll control from compressor bleed. Blowing boundary-layer control is used to increase tail and elevator effectiveness during transition. Acceleration to wing-supported flight is achieved by tilting the aircraft. Further details of the aircraft are presented in reference 9.

Ryan XV-5A

The XV-5A (fig. 5) is powered by two jet engines which drive two fans in the wing and one in the nose for VTOL lift. These engines provide direct thrust for cruise. VTOL roll control is provided by lift-fan thrust modulation, yaw control by differential operation of wing-fan exit louvers, and pitch control by nose-fan thrust modulation. Acceleration to wing-supported

flight is provided by deflecting the main fan flow aft with the fan exit louvers. Further details of the aircraft are presented in reference 10.

TESTING

The wind-tunnel tests were all performed in the Ames 40- by 80-Foot Wind Tunnel with similar test setups (e.g., see figs. 1-5) and procedures. However, the flight tests were carried out by various agencies which had various specific objectives. In none of the wind-tunnel or flight tests was the prime objective to correlate wind-tunnel and flight-test results; thus the amount of data available for this correlation is limited.

Wind-Tunnel Testing

Aerodynamic and static-stability and control characteristics were all explored near balanced flight conditions. At discrete airspeeds, from 0 to wing-supported flight speed, data were obtained with lift equal to weight, drag equal to thrust, and pitching moment equal to zero. Then angle of attack, angle of sideslip, power setting, and the various control settings were varied to determine the effect of each variable on aircraft characteristics. This type of wind-tunnel testing is the fastest way of obtaining pertinent data on flying characteristics.

Flight Testing

Unless otherwise noted, the flight-test results were obtained with steady-state conditions for approximately level flight or hovering and were further limited to avoid deep penetration into known problem areas. Flight work with the XV-3 and VZ-3 was done at Ames, and an Ames representative was on hand during XV-5A flight tests, so the problems of coordinating and interpreting data were easily solved. The contractors supplied the applicable flight-test data that had been reduced for the XC-142 and the XV-4A, which resulted in a smaller amount of data being available for correlation because the major interests of the contractors were not wind-tunnel and flight-test correlations.

RESULTS AND DISCUSSION

Correlation of Wind-Tunnel and Flight-Test Results

Representative aerodynamic data from wind-tunnel and flight tests for the five aircraft are compared in this section. Unless otherwise noted, none of the wind-tunnel data are corrected for wall effects. In most cases the comparison is made at steady-state level-flight or hovering conditions (lift equal to weight, thrust equal to drag).

XV-3.- Power required for level flight, fuselage angle, and longitudinal control position for trim both in flight and in the wind tunnel are shown as functions of airspeed in figure 6. Power required as a function of airspeed shows excellent agreement, but angle-of-attack and longitudinal-control data show scatter. Since accuracy in setting longitudinal control was $\pm 1^\circ$ in the wind tunnel, and angle of attack is difficult to measure accurately in slow-speed flight, the agreement between the two sets of data is considered good. Although the aircraft span was large with respect to the tunnel width (table I), the disk loading was low (about 5 psf) so that the wake deflection angle due to airspeed was large and the adverse effects of model size on wind-tunnel wall effects were small.

VZ-3.- Similar results (power required, angle of attack, and longitudinal control) are presented in figure 7 for this deflected slipstream aircraft. Again, power required for level flight showed excellent agreement between wind tunnel and flight. A 23-percent increase in horizontal-tail area, added after the wind-tunnel tests, may have contributed to the fuselage angle of attack for trim being about 1° greater in flight and the nose-down elevator for trim being about 2° less in flight than in the wind tunnel. This aircraft was small with respect to the wind tunnel and the disk loading was moderate (20 psf) so that wind-tunnel wall effects were small.

The small discrepancies noted between wind-tunnel and flight-test results did not prevent adequate assessment of the aircraft performance, stability, and control.

XC-142.- Wing incidence angle for trimmed, level flight is presented in figure 8 as a function of airspeed. Wind-tunnel and flight-test results agree within 5° for the wing-tilt angle required for 30-knots airspeed and within 2° for 55-knots airspeed.

Descent rates obtained in flight and predicted from wind-tunnel data are presented in figure 9 as a function of airspeed for several aircraft configurations. The flight-test data fall into two curves, one is the descent rate for buffet onset, and the other is the maximum descent rate as defined by small lateral-directional oscillations. The descent rates for buffet onset seem to agree with wind-tunnel data up to 45-knots airspeed at the higher wing-tilt angles. At higher airspeeds and lower wing-tilt angles the maximum descent rates obtained in flight are much greater than those estimated from the wind-tunnel data. The descent rates estimated from the wind-tunnel data are based on when $C_{l_{max}}$ was first attained, or, in the cases noted, on the maximum angle of attack for which data are available. It is unlikely that wind-tunnel wall effects are responsible for the discrepancy because of the better correlation of flight and wind-tunnel results at low speed. A more likely cause of the difference is either the low maximum lift of the model, or the aircraft's flying beyond $C_{l_{max}}$ with no adverse effects. Model scale and the reduction in test airspeed caused by the low installed power combined to reduce Reynolds number to one-third of the full-scale value for a given value of thrust coefficient; this caused model Reynolds number to be in the region where maximum lift can be significantly affected, and can thus affect the correlation.

Based on present knowledge, agreement is fair for trimmed level flight but poor for allowable descent angles.

XV-4A.- Flight-test data were limited for this aircraft. Data are available only for transitions during which the aircraft was decelerating. Figure 10 shows the longitudinal acceleration, angle of attack, and elevator position as functions of airspeed during a transition. The angle of attack and elevator position for trim estimated from the wind-tunnel data to produce the equivalent deceleration in level flight are included on the figure. Angle of attack generally agreed to within 1° , but elevator position differed by 4° to 7° (12 percent of maximum travel). The reason for the relatively poor correlation of elevator angle is not clear. The aircraft tested in the wind tunnel was not the same aircraft that supplied the flight-test data, so some of the difference could be based on differences in rigging or effectiveness of horizontal-tail boundary-layer control.

Both conventional wind-tunnel wall corrections and Heyson's corrections were applied to the XV-4A wind-tunnel data in an attempt to improve correlation with flight. Figure 11 shows the XV-4A angle of attack for the same deceleration as in figure 10, as calculated from uncorrected wind-tunnel data (level flight was assumed), and from wind-tunnel data with conventional corrections and with Heyson's corrections (including the effects of finite span). Conventional corrections increased the angle-of-attack discrepancy from 1° to about 1.5° . Heyson's corrections increased the discrepancy slightly.

XV-5A.- Relative power, angle of attack, fan exit louver angle, and longitudinal stick position required for balanced flight are presented as functions of airspeed in figure 12. The power required for level flight decreased as airspeed increased, indicating that, rather than a "suckdown" effect, lift for a constant power setting increased with airspeed. Based on the results in reference 11, a reduction of lift with airspeed would be expected for constant power. Although the flight-test data show considerable scatter due to small accelerations, the agreement between wind tunnel and flight is good. It should be noted that this aircraft was nearly twice the size of the XV-4A, and lifting-element loading was about the same. The largest discrepancy between flight and wind-tunnel tests is in longitudinal stick position; this discrepancy is about 1° , or 3 percent of the total stick travel.

Subsequent to these flights, the fairings at the wing-fan hub between the rotor blades were removed, changing fan performance so that more power and larger fan-exit louver angles were required for a given flight speed. Flight-test data with the revised fan configuration were obtained at constant airspeed and several angles of attack. The longitudinal stick position for trim as a function of angle of attack is presented in figure 13 for three airspeeds. Good correlation is evident at 36 and 50 knots. Agreement is poor at 70 knots, indicating the static stability in the wind tunnel was different from that measured in flight; the discrepancy would be further increased by wall corrections. At least a part of the failure to correlate at 70 knots is due to the sensitivity of pitching moment to exit louver angle at this airspeed. Because the fairings had been removed, the louver angles in flight were 1.5° to 7° greater than for the wind-tunnel results shown in figure 13.

The XV-5A wind-tunnel tests showed an instability with angle of attack over part of the angle-of-attack range, the particular angle of attack for instability being a function of the nose-fan thrust-modulator position. Tests with and without nose-fan thrust modulation indicated that the instability was caused by a reduction of tail effectiveness due to the flow from the nose fan with the thrust modulated to give a large nose-down control moment. In the flight tests, aircraft angle of attack was increased until the tail angle-of-attack indicator registered turbulent flow; the test was then terminated. The consequent flight-test angle-of-attack boundary and the wind-tunnel angle of attack for instability are presented in figure 14. Considering the qualitative nature of the flight-test data, agreement is good, and it appears that flow conditions at the tail were adequately simulated in the wind tunnel.

The effect of wind-tunnel wall corrections on the XV-5A wind-tunnel and flight correlation is shown in figure 15. The effect of both finite span and side-by-side lifting elements were included for Heyson's corrections. In this case conventional wall corrections were nearly as large as Heyson's corrections, but they did not improve the correlation; however, the effect on exit louver angle required for trimmed flight was small. The most significant effect was on power required; wall-effect corrections amounted to a 10-percent increase over that measured in flight.

Summary of test results.- The correlation between flight-test and wind-tunnel results for these five aircraft demonstrates the accuracy achieved in V/STOL wind-tunnel testing with aircraft-tunnel size ratios approaching those used for wind-tunnel tests of conventional aircraft. Correlation with uncorrected wind-tunnel data was good, with the exception of the XC-142 model. It was also shown that for the two cases examined, applying wind-tunnel wall corrections calculated by the available methods degraded the correlation, indicating a need for more theoretical work on wind-tunnel wall corrections for aircraft with localized, high-disk-loading lifting elements. For the majority of correlations of wind tunnel with flight, the conditions considered were for lift equal to weight, and thrust equal to drag. Wall effects were smaller for these flight conditions than when aircraft drag was unbalanced, because the lifting-element wake is deflected downstream.

Wall-Effect Parameters

Present test results.- The preceding section examined the accuracy of uncorrected wind-tunnel data for several aircraft of widely differing characteristics and sizes with respect to the wind tunnel. Model-tunnel sizing parameters for the aircraft that demonstrated acceptable correlation can be related to aerodynamic parameters in order to indicate acceptable V/STOL model sizing. According to reference 3, the pertinent model-tunnel sizing parameters are the ratio of the area of the VTOL lift generators to wind-tunnel cross-sectional area, A_L/A_T , for VTOL concepts where the majority of the lift is supplied by the lifting elements, and the ratio of momentum area to tunnel cross-sectional area, A_M/A_T , for concepts where the lift is distributed across the wing span. Study of reference 1 also shows that lifting-element wake-deflection angle, which is a function of disk loading at a given airspeed (wake deflection angle = $f(V/V_j) = f(V/\sqrt{T_F})$), is another important parameter.

Disk loading is an important parameter for all V/STOL aircraft and provides a common basis for comparison. Accordingly, both lifting-element and momentum area ratios are plotted versus disk loading in figure 16 for the five test aircraft.¹ Both suggested area ratios are included for all five aircraft. The XV-3 and XV-5A represent extremes of the ratio of model size to wind-tunnel size that have small wall effects. Narrow shaded areas have been drawn connecting their data points to indicate a possible size-ratio boundary for small wall effects. Ratios of model to wind-tunnel size that fall below these areas indicate acceptable model sizing. The point for the XC-142, which appears above the shaded area, leaves unresolved questions concerning the correlation, and it may be that this model is too large for the wind tunnel. The wind-tunnel and flight correlation was acceptable for the VZ-3 and XV-4A, and the data points for these aircraft fall below the shaded area. The tentative nature of the location and shape of the shaded areas on figure 16 should be emphasized.

The narrow shaded areas shown in figure 16 connect points for two aircraft tested in the wind tunnel at different minimum speeds; the aircraft with the lower disk loadings showed good agreement to speeds as low as 20 knots; whereas for those with higher disk loadings it was difficult to get reliable data below 30 knots because blockage and recirculation made it difficult to achieve steady test conditions. Additional data may show that separate 20- and 30-knot boundaries should be drawn on the figure, rather than the single boundary for the two airspeeds. The boundaries drawn on figure 16 probably approximate a practical test boundary because the need for wind-tunnel data between 0 and 30 knots depends on disk loading; aircraft with low disk loadings will fly a larger percentage of the time at low speeds and will be more sensitive to gusts or small maneuver velocities than aircraft with higher disk loadings at the lower forward speeds.

Comparison of boundaries with other results.- Small-scale results, from testing the same model in different wind-tunnel test sections (refs. 2 and 5), were analyzed in an attempt to document further the boundaries in figure 16. For all models, the ratio of model to tunnel size in the smallest test section approached conventional values, and test conditions were near the shaded boundary areas of figure 16. Discrepancies in lift of 6 percent or less (when evaluated with thrust equal to drag), caused by differing test-section size, are considered to be small wall effects and of the same order as the accuracy of the data in the preceding wind-tunnel flight-test correlation. The uncorrected tilt-wing data from the 7- by 10-foot wind tunnel (ref. 5) were well within the 6-percent margin for balanced flight at low speed. Uncorrected lift data from a helicopter rotor in large and small test sections (ref. 2) also agreed within 6 percent for balanced flight at low speed. Reference 5 did not present balanced flight data for the lift-fan configurations, so it was necessary to use data that correspond to large aircraft decelerations. Unlike the other two models, the two lift-fan configurations in the smallest

¹Other common parameters, such as the ratio of disk loading to dynamic pressure, velocity ratio V/V_j , or wake deflection angle, were considered but were not used because of the assumptions required for their calculation. Furthermore, these parameters obscure the wide range of disk loading represented by the composite data from the several aircraft.

test sections showed sizable lift errors. It was thus necessary to plot both the fan-in-fuselage and fan-in-wing lift errors in the various wind-tunnel test sections as functions of ratio of model to wind-tunnel size in order to determine the area ratio for a 6-percent lift discrepancy. This method introduced a further uncertainty because the wind tunnels had different width-to-height ratios. The appropriate ratios of model to wind-tunnel size for these four models are compared with the wind-tunnel flight-test correlation boundaries on figure 17. The two model tests with the lower disk loadings indicate no conflict between the full-scale results (the shaded areas on fig. 17) and the model tests; however, for the models with the higher disk loadings a decided discrepancy is evident. At least a partial explanation is failure to balance model drag, so that the wake deflection angle was less for these models than for the similar aircraft. If Heyson's corrections are taken as an indication of the importance of wake deflection angle, balancing the drag can reduce the calculated wall corrections to as little as 50 percent of the values with the drag unbalanced. A change in this direction would tend to reduce the discrepancy between the small-scale results with high disk loading and the correlation of wind-tunnel and flight-test data. Another possible cause of the discrepancy is the large span relative to wind-tunnel width; this subject is discussed in the next section.

Although some of the results presented in reference 5 disagree with the results presented here for model-tunnel sizing parameters, adequate reasons for the disagreement exist. For the conditions considered in the present report (i.e., realistic flight conditions and allowable errors no larger than data-measurement errors), the ratios of model to wind-tunnel size, as indicated by the boundary lines on figure 16, which are larger than previously considered usable, should give acceptable wind-tunnel results for V/STOL model testing.

Test-section geometry. - The correlation of wind-tunnel and flight-test results is based on tests in a wind tunnel with a 2-to-1 width-height ratio, which is larger than that in any of the small-scale tests. This test-section geometric parameter has a direct bearing on span-to-tunnel width ratios, which is an important parameter in conventional wind-tunnel wall corrections and may also be important for V/STOL model testing. This ratio is presented in figure 18 as a function of disk loading for the aircraft in the correlation of wind-tunnel and flight-test data (solid symbols) and for the models in references 2 and 5 installed in their smallest test section (open symbols). The aircraft and models that indicated insignificant corrections have conventional ratios of span to wind-tunnel width at low disk loadings and relatively small span-to-width ratios at high disk loadings. The two small-scale lift-fan models that indicated large wind-tunnel wall corrections had larger span-to-width ratios than the comparable aircraft. These results suggest that another boundary area in addition to those in figure 16, indicating acceptable ratios of span-to-tunnel width, may be appropriate to specify the effects of test-section geometry when sizing a V/STOL model. For certain V/STOL concepts where the propulsive system span extends considerably beyond the span of the wing, as on compound helicopters or tilt rotor aircraft or where the propulsive system extends only over a small part of the wing span, as on fan-in-wing systems, the lifting element span may be a factor along with wing span for determining the magnitude of wall effects or model size. The effects

of wind-tunnel cross-section geometry on wall effects should be studied experimentally since they may significantly influence V/STOL wind-tunnel data.

CONCLUDING REMARKS

In order to obtain satisfactory data from V/STOL wind-tunnel testing in the low-speed flight range, it is necessary to resolve the conflict in model sizing caused by the need to minimize both wall effects and scale effects. In reference 5, scale effects were shown to be larger than the effect of Heyson's corrections in some cases, but in other cases (the XV-4A, 0.18 scale, $A_L/A_T = 0.01$) were shown to be negligible. Thus careful planning of test programs is required in order to minimize the possibility of obtaining erroneous or misleading test data.

The results of correlating the aerodynamic data obtained in wind-tunnel and flight investigations of several V/STOL concepts have given an indication of gross tentative boundaries that should be observed for three sizing parameters of model geometry to wind-tunnel geometry. Experience may indicate that these boundaries are optimistic in model size in other width-to-height ratio wind-tunnels or apply only to the specific type of aircraft considered in the correlation. Observation of the indicated boundaries should yield data of reasonable accuracy and prove to be useful for predicting aerodynamic characteristics and trends related to changes in configuration. However, the data may be lacking in absolute precision with regard to angle of attack and effects of distortion, particularly at velocities below 20 to 30 knots, depending on the disk loading of the propulsive system. For testing at lower airspeeds or at higher disk loadings than considered herein, smaller ratios of model to wind-tunnel size will be necessary; whereas for STOL testing larger values of the sizing ratios should be acceptable. The models should be as large as permissible because Reynolds number effects can be critical for inlets, high-lift devices, and the characteristics of propellers, fans, and compressors. The flow distribution of the lifting elements should approximate full-scale characteristics to match secondary flow effects, and disk loading should approximate full-scale disk loading in order to obtain adequate data over the airspeed range of interest and provide an acceptable Reynolds number when matching full-scale thrust coefficients. For a given wing loading, conditions closely corresponding to realistic flight values of acceleration and deceleration reduce wind-tunnel wall effects and enable use of larger models in wind tunnels. Instrumentation sufficient for determining the performance of the various model components, including the lifting elements, is useful in detecting substandard performance of the components due to low Reynolds number or failure to realistically simulate the aircraft or lifting-element disk loading.

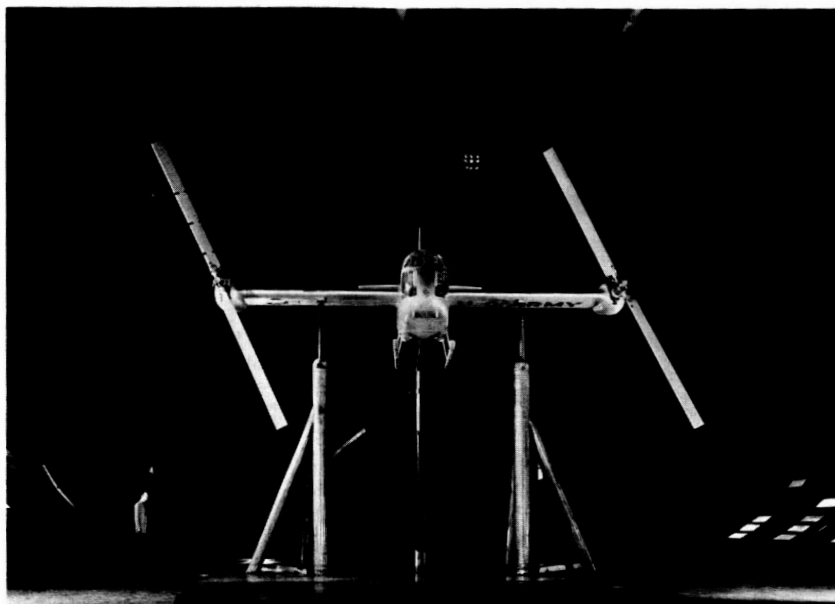
REFERENCES

1. Heyson, Harry H.: Linearized Theory of Wind-Tunnel Jet-Boundary Corrections and Ground Effect for VTOL-STOL Aircraft. NASA TR R-124, 1962.
2. Lee, Jerry Louis: An Experimental Investigation of the Use of Test Section Inserts as a Device to Verify Theoretical Wall Corrections for a Lifting Rotor Centered in a Closed Rectangular Test Section. Thesis for Masters Degree, University of Washington, 1964.
3. Davenport, Edwin E.; and Kuhn, Richard E.: Wind-Tunnel Wall Effects and Scale Effects on a VTOL Configuration With a Fan Mounted in the Fuselage. NASA TN D-2560, 1965.
4. Grunwald, Kalman J.: Experimental Study of Wind-Tunnel Wall Effects and Wall Corrections for a General-Research V/STOL Tilt-Wing Model With Flap. NASA TN D-2887, 1965.
5. Powered-Lift Aerodynamics Section Staff: Wall Effects and Scale Effects in V/STOL Model Testing. Paper at AIAA-Navy Aerodynamic Testing Conference, 1964.
6. Koenig, David G.; Greif, Richard K.; and Kelly, Mark W.: Full-Scale Wind-Tunnel Investigation of the Longitudinal Characteristics of a Tilting-Rotor Convertiplane. NASA TN D-35, 1959.
7. James, Harry A.; Wingrove, Rodney C.; Holzhauser, Curt A.; and Drinkwater, Fred J., III: Wind-Tunnel and Piloted Flight Simulator Investigation of a Deflected-Slipstream VTOL Airplane, the Ryan VZ-3RY. NASA TN D-89, 1959.
8. Deckert, Wallace H.; Page, V. Robert; and Dickinson, Stanley O.: Large-Scale Wind-Tunnel Tests of Descent Performance of an Airplane Model With a Tilt Wing and Differential Propeller Thrust. NASA TN D-1857, 1964.
9. Anon.: Lockheed Hummingbird Preliminary Aircraft Specification. Lockheed Document ER-5180M, May 1961.
10. Anon.: Lift-Fan Flight Research Aircraft Program, Airplane Detail Specification. Specification 118A, General Electric Company, Flight Prop. Lab. Dept., Cincinnati, Ohio, April 1963.
11. Spreemann, Kenneth P.: Induced Interference Effects on Jet and Buried-Fan VTOL Configurations in Transition. NASA Conference on V/STOL Aircraft, 1960.

TABLE I.- AIRCRAFT GEOMETRY WITH RESPECT TO THE WIND TUNNEL

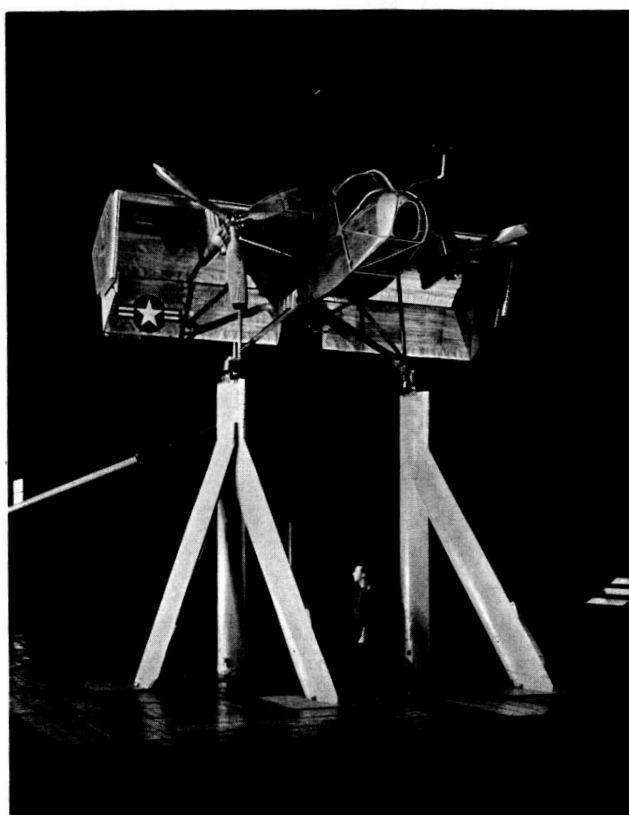
Aircraft	Type	$\frac{A_L}{A_T}$	$\frac{A_M}{A_T}$	$\frac{b}{b_T}$	$\frac{T}{A_L}$	Applicable figures
XV-3	Tilt rotor	0.291	0.758	0.656	5.6	1, 6
VZ-3	Vectored slipstream	.046	.151	.292	19.9	2, 7
XC-142	Tilt wing	.095	.451	.506	50*	3, 8, 9
XV-4A	Jet ejector	.0077	.186	.325	300	4, 10, 11
XV-5A	Lift fan	.0149	.244	.372	275	5, 12, 13, 14, 15

*Full-scale disk loading only; model disk loading was 15 lb/sq ft.



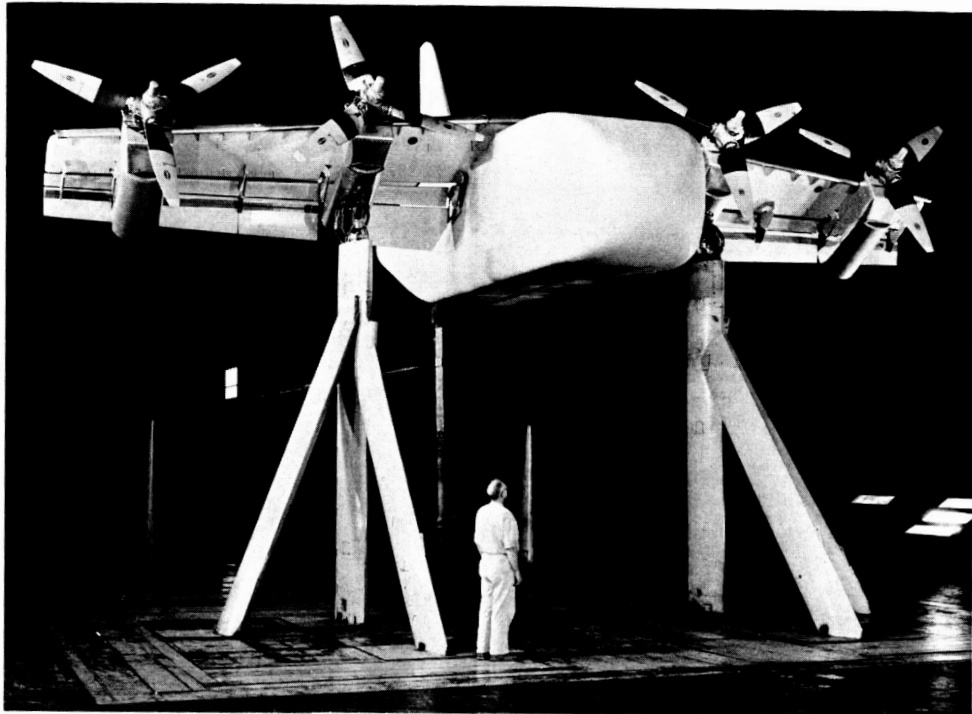
A-23164

Figure 1.- The Bell XV-3 mounted in the Ames 40- by 80-Foot Wind Tunnel (aircraft wind-tunnel geometry in table I).



A-23991

Figure 2.- The Ryan VZ-3 mounted in the Ames 40- by 80-Foot Wind Tunnel (aircraft wind-tunnel geometry in table I).



A-29909

Figure 3.- The LTV XC-142 model mounted in the Ames 40- by 80-Foot Wind Tunnel (model wind-tunnel geometry in table I).



A-33193

Figure 4.- The Lockheed XV-4A mounted in the Ames 40- by 80-Foot Wind Tunnel (aircraft wind-tunnel geometry in table I).



A-35394-11

Figure 5.- The Ryan XV-5A mounted in the Ames 40- by 80-Foot Wind Tunnel (aircraft wind-tunnel geometry in table I).

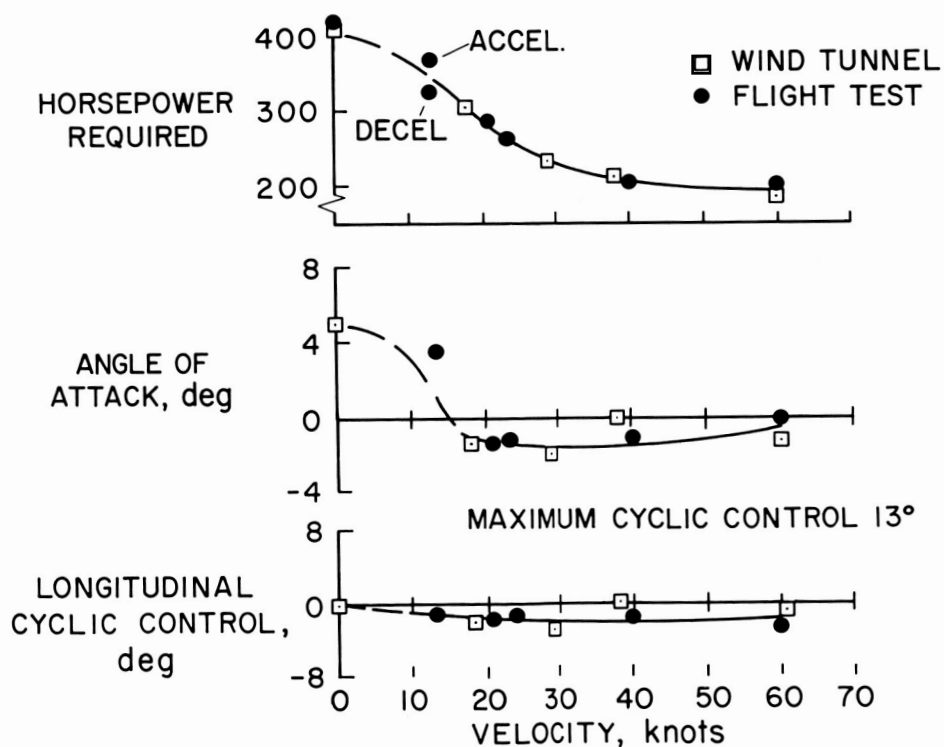


Figure 6.- Balanced, level-flight characteristics of the XV-3 convertiplane as measured in the wind tunnel and in flight.

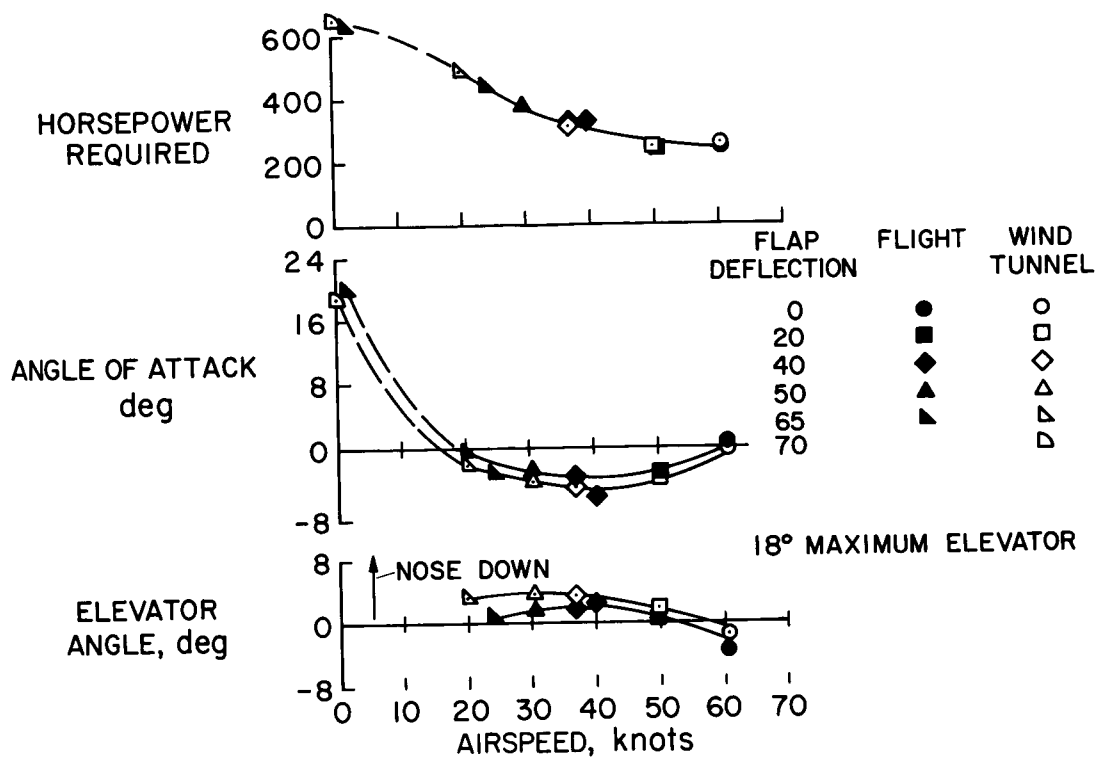


Figure 7.- Balanced, level-flight characteristics of the VZ-3 aircraft as measured in the wind tunnel and in flight.

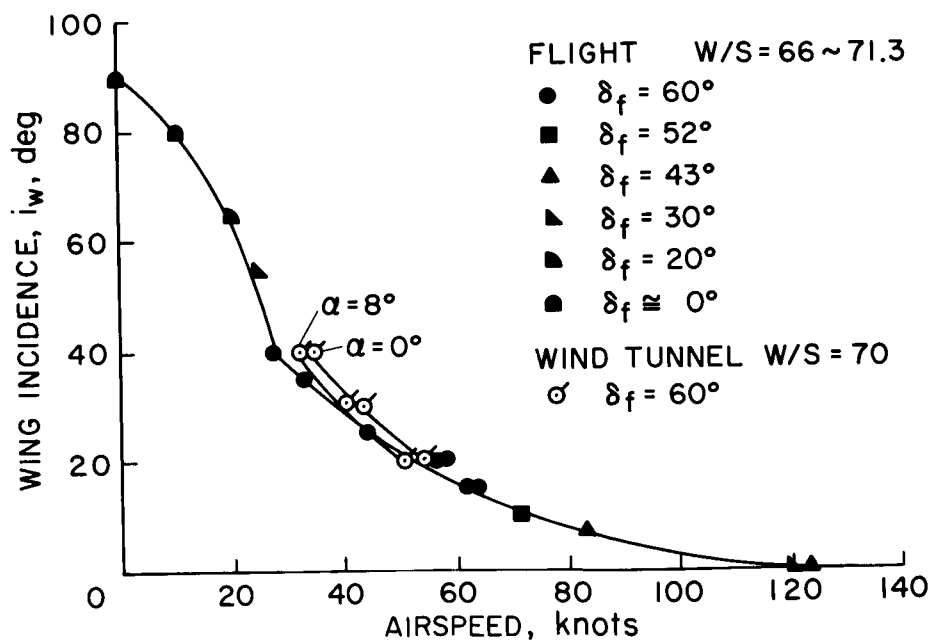


Figure 8.- Wing-tilt angle for balanced, level flight of the XC-142.

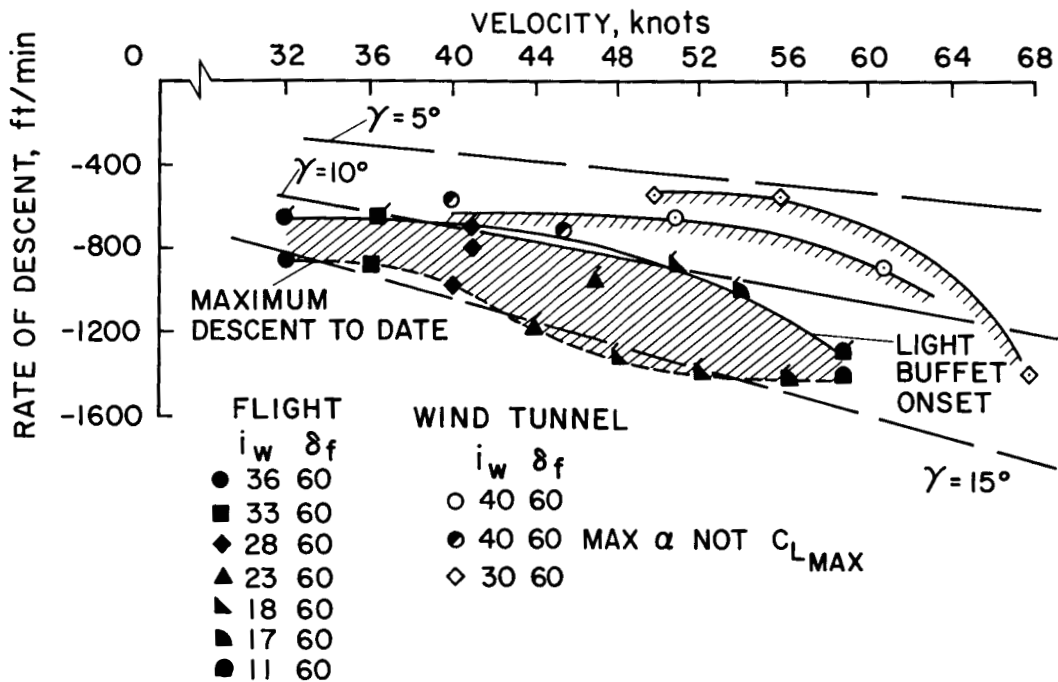


Figure 9.- Descent boundaries for the XC-142.

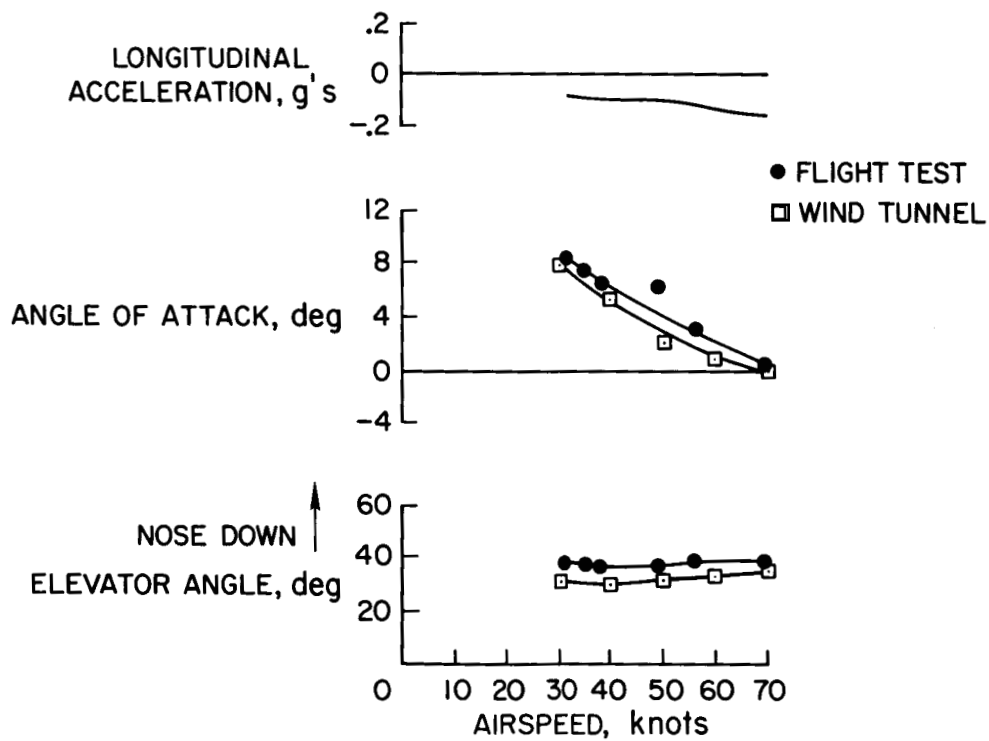


Figure 10.- Characteristics of the XV-4A.

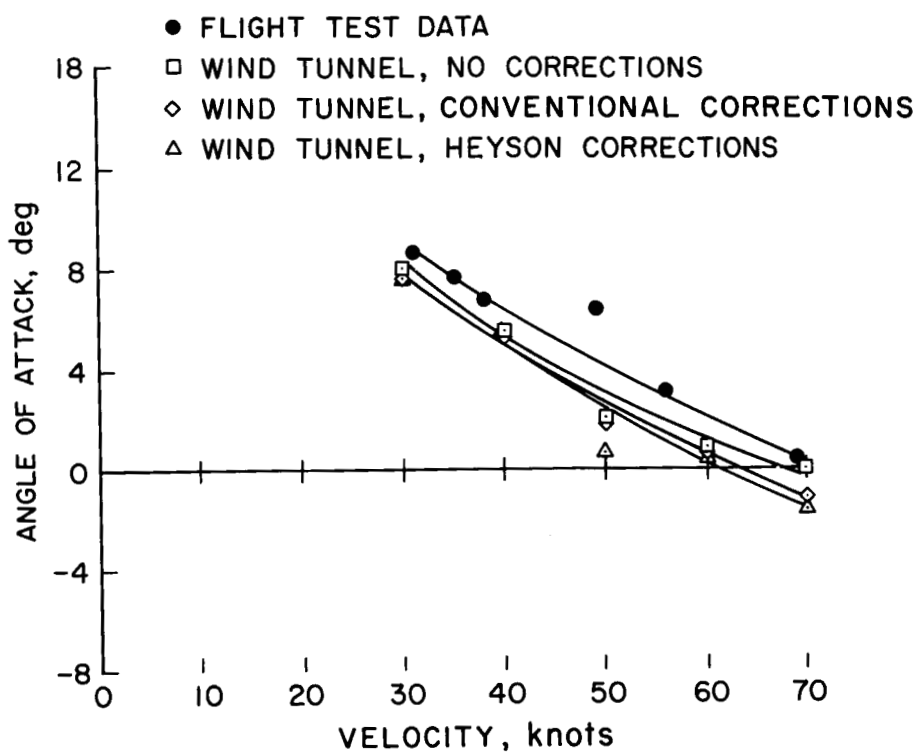


Figure 11.- The effect of wind-tunnel wall corrections on the correlation between wind-tunnel and flight-test results for the XV-4A.

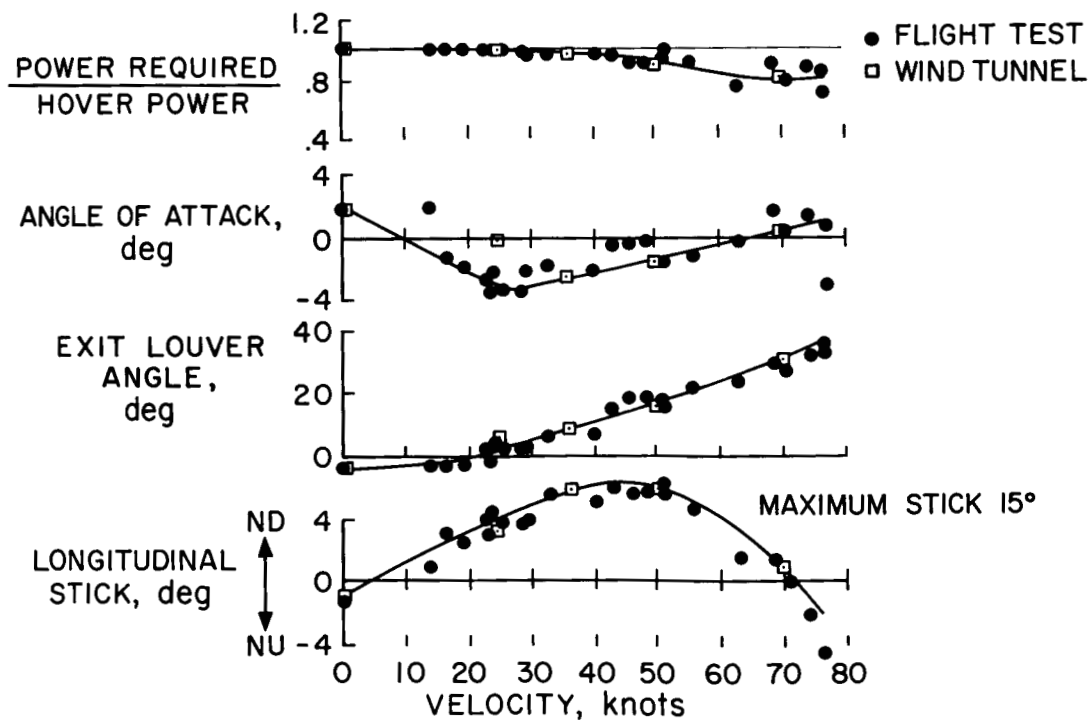


Figure 12.- Balanced, level flight characteristics of the XV-5A as measured in the wind tunnel and in flight.

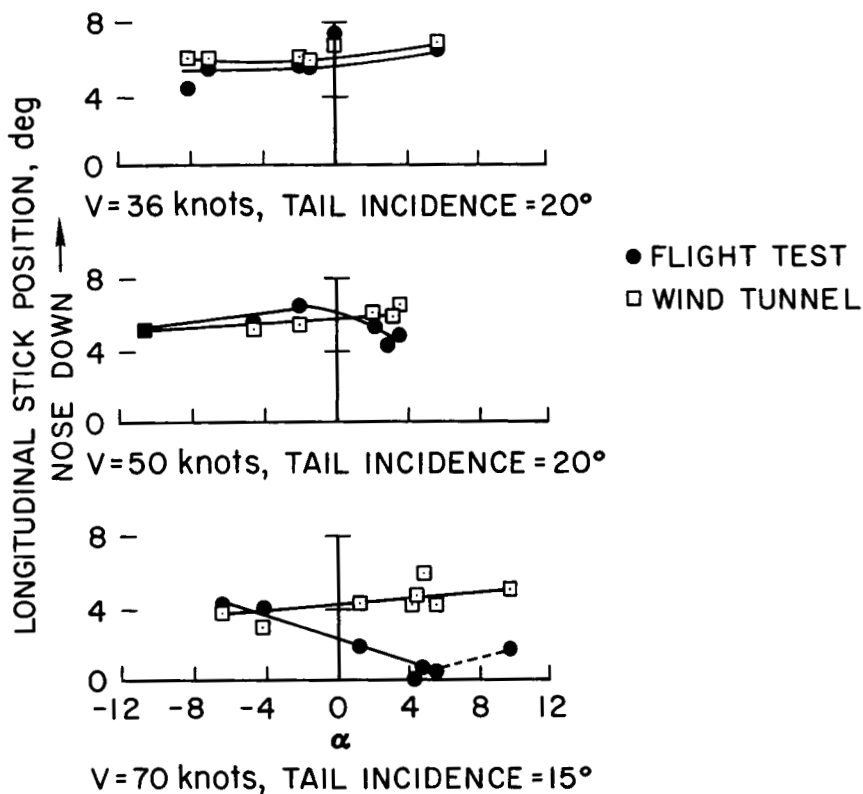


Figure 13.- The variation with angle of attack of longitudinal stick position for trim for the XV-5A aircraft in flight and in the wind tunnel.

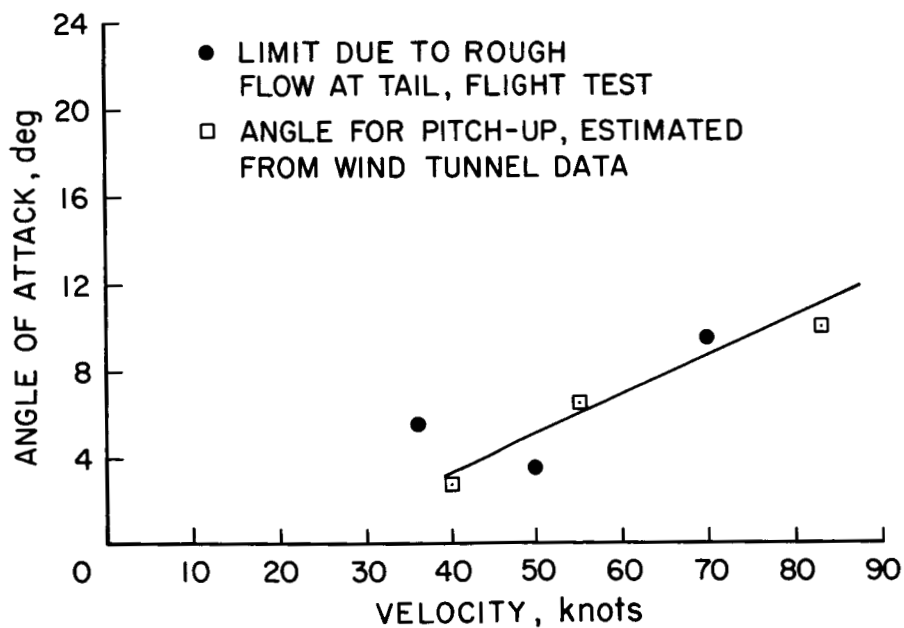


Figure 14.- Angle of attack for instability or rough flow at the tail of the XV-5A in flight and in the wind tunnel.

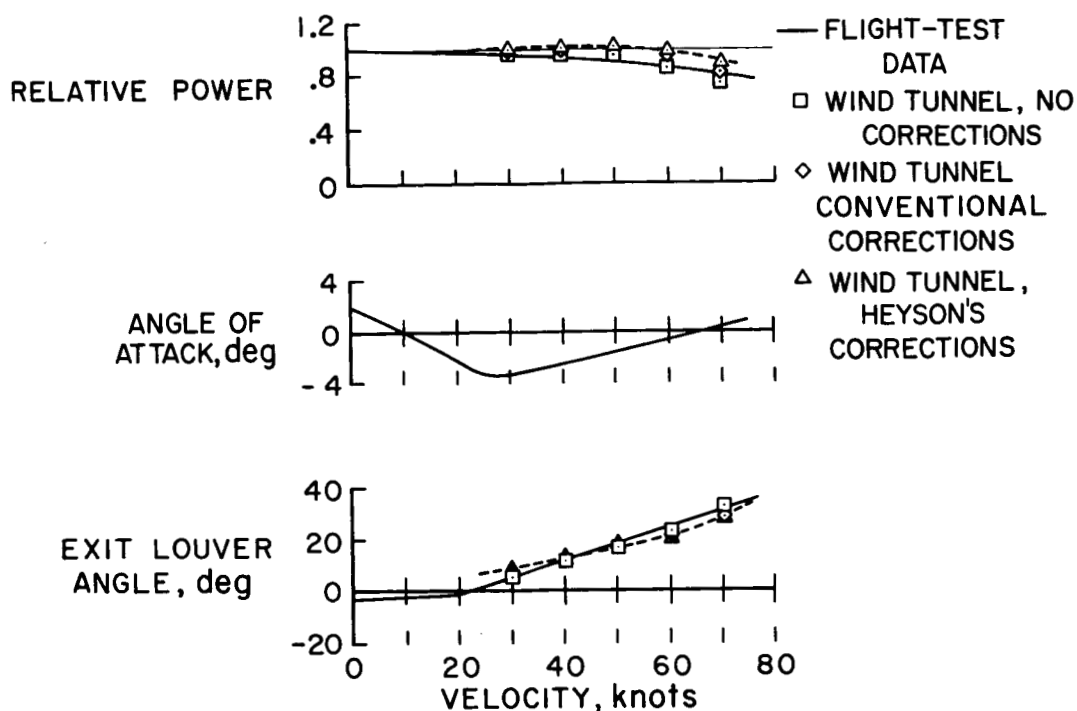


Figure 15.- Effect of wind-tunnel wall corrections on correlation between wind-tunnel and flight-test results for the XV-5A aircraft.

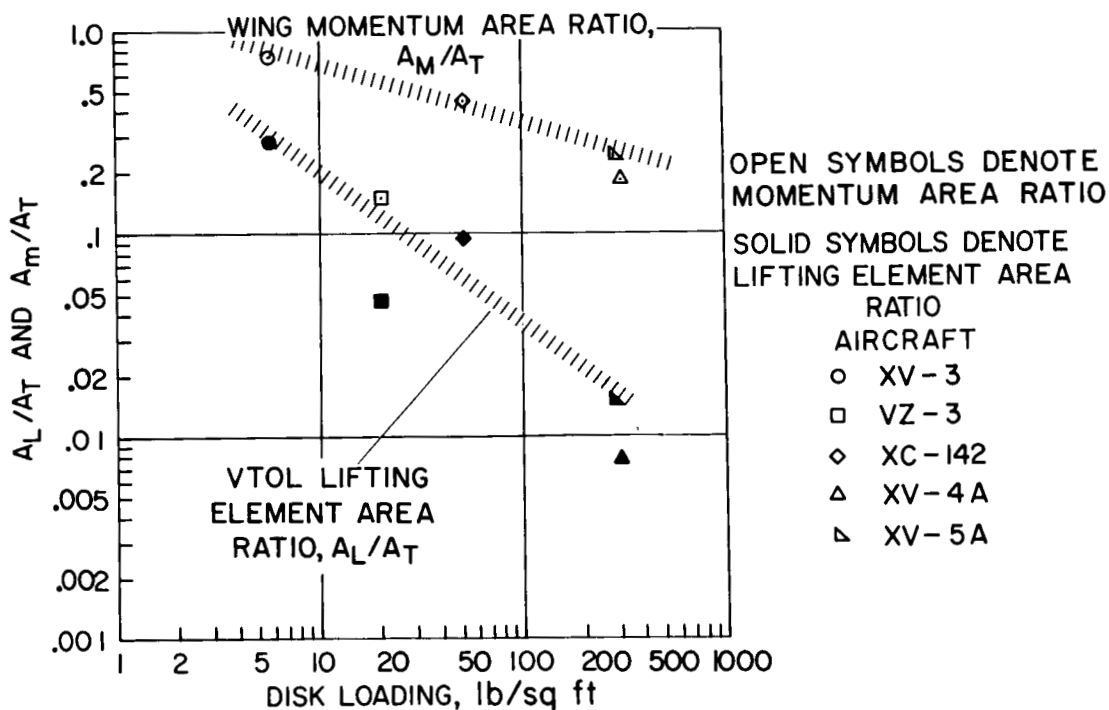


Figure 16.- The variation of the ratio of aircraft to wind-tunnel size with disk loading for aircraft tested in the wind tunnel at 20 to 30 knots airspeed.

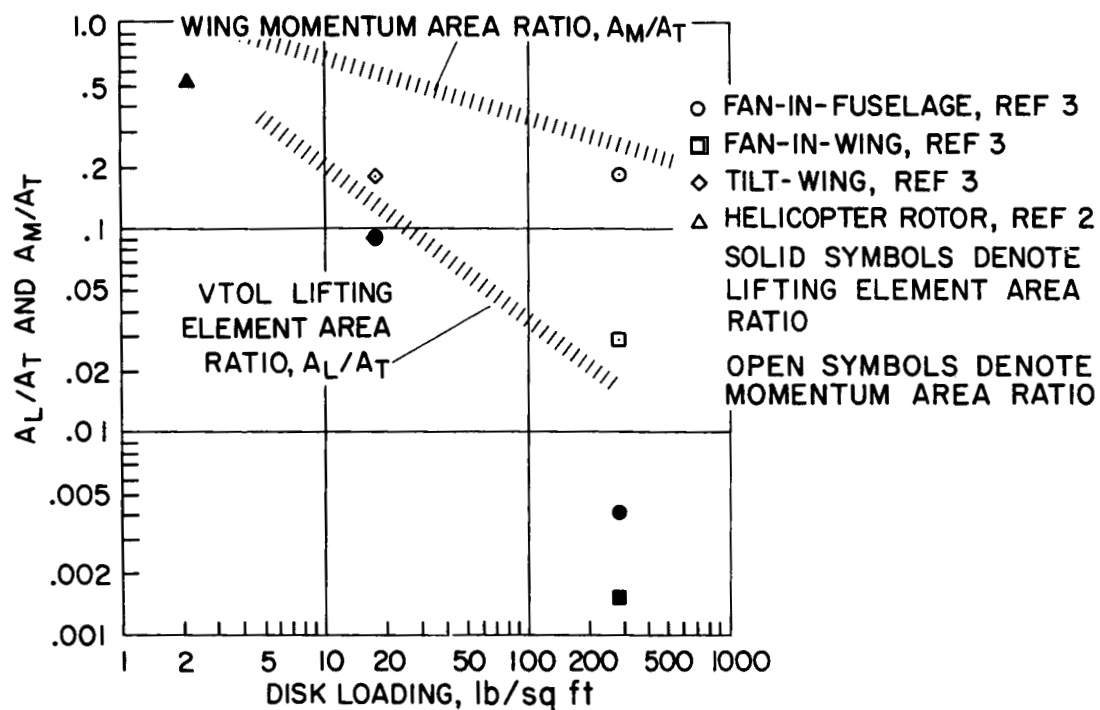


Figure 17.- The variation of the ratio of small-scale model to wind-tunnel size with disk loading.

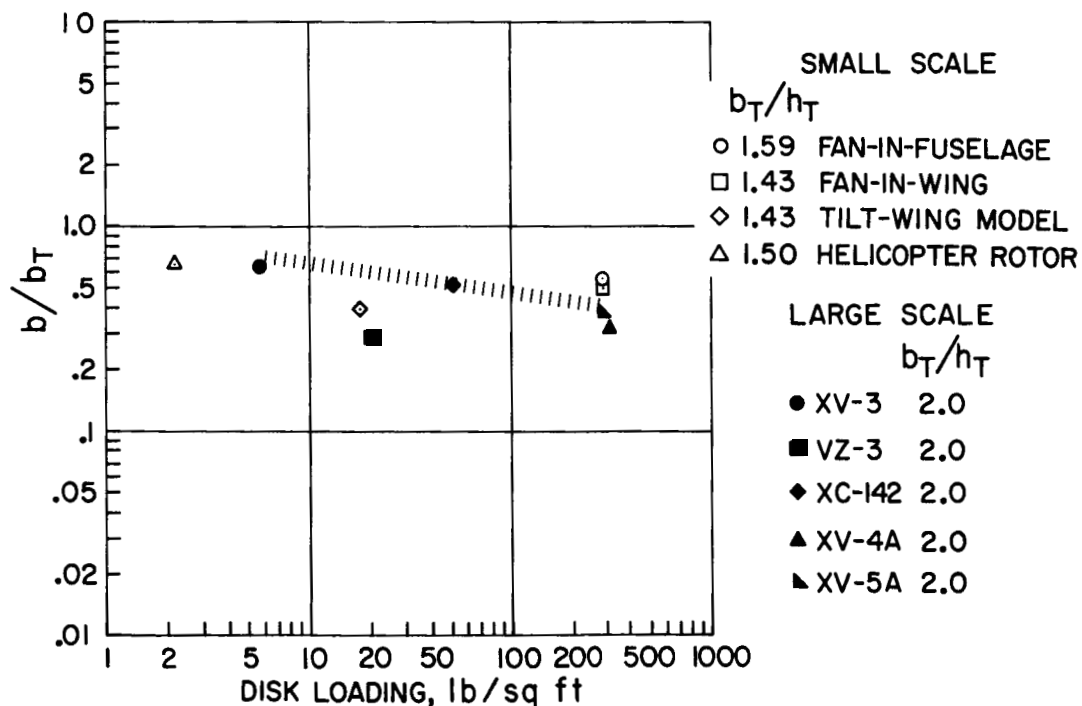


Figure 18.- The ratio of aircraft and model span to wind-tunnel width.